COMMUNICATION

ChemComm
www.rsc.org/chemcomm

Molecular recognition for stable organic radicals — 2-(6-uradinyl)-4,4,5,5-tetramethyl-4,5-dihydro-1*H*-imidazole-1-oxyl†

Patrick Taylor, Paul R. Serwinski and Paul M. Lahti*
Department of Chemistry, University of Massachusetts, Amherst MA 01003, USA.
E-mail: lahti@chem.umass.edu

Received (in Columbia, OH, USA) 12th March 2003, Accepted 25th April 2003
First published as an Advance Article on the web 19th May 2003

Stable radical 2-(6-uradinyl)-4,4,5,5-tetramethyl-4,5-dihydro-1*H*-imidazole-1-oxyl shows antiferromagnetic spin pairing with $2J/k = -14$ K, attributable to a close contact between unpaired spin density on the imidazole-type nitrogen atoms; hydrogen bonds aid dimer formation, but do not appear to play an eletronic role in the magnetic behaviour.

The use of hydrogen-bonding as a crystal-engineering scaffold has been utilized in a number of cases to attempt to control the solid state intermolecular exchange interactions of organic free radicals.[1] In an example using a biology-inspired motif, Veciana *et al.*,[2] described the synthesis, crystal analysis, and magnetic properties of 2-(5-uradinyl)-4,4,5,5-tetramethyl-4,5-dihydro-1*H*-imidazole-1-oxide-3-oxyl (5-Ur-NN, **1**). Only a small amount of spin density was observed on the uradinyl ring in **1**. This is probably due to two factors. Nitronylnitroxides do not delocalize spin much beyond the conjugated ON–C–NO moiety, and **1** exhibits a high biannular torsional angle (64.9°).

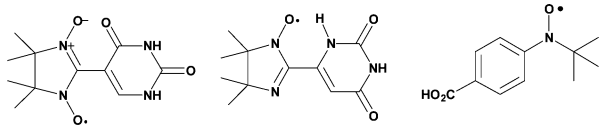

1 **2** **3**

The relationship of the magnetic interactions to the crystal packing was not entirely clear in **1**. By making a more planar analogue of **1**, we hoped to improve crystal stacking, and possibly to increase radical to uradinyl spin delocalization. In this article, we report the synthesis, crystallography, and magnetic analysis of 2-(6-uradinyl)-4,4,5,5-tetramethyl-4,5-dihydro-1*H*-imidazole-1-oxyl (6-Ur-NN, **2**).

Commercial 6-methyluracil was oxidized[3] to 6-formyluracil, condensed[4] with 2,3-bis(hydroxylamino)-2,3-dimethylpropane hydrogen sulfate, then directly oxidized with aqueous sodium periodate and purified to give **2** as a brick red powder that appears indefinitely stable to ambient conditions. The radical was characterized‡ by elemental analysis, crystallography, electron spin resonance and FTIR spectroscopy. The seven-line solution electron spin resonance (ESR) spectrum of **2** showed no resolvable hyperfine coupling from atoms other than the two nonequivalent nitrogens. Variable temperature and frozen matrix (2 : 1 toluene/hexanes) ESR were obtained, but we observed no triplet biradical peaks attributable to solution phase dimer formation. Apparently, the aggregates are too few or too disorganized to exhibit solution biradical ESR spectra analogous to those recently seen for radical **3**.[5] However, we did observe dimers, trimers, and higher aggregates in electrospray impact mass spectra obtained for **2**. For example, in methanol we obtained peaks at *m*/*z* 252.3, 503.4 and 776.4 for $(\mathbf{2} + H)^+$, $(\mathbf{2}_2 + H)^+$, and $(\mathbf{2}_3 + Na)^+$ (sodium ions are from the sample's glassware environment), and even further clusters up to at least $(\mathbf{2}_6 + Na)^+$. These cluster peaks were not formed in aqueous acetic acid, presumably due to disruption of hydrogen-bonding under these conditions. We note that UV-vis based evidence of some form of aggregation has also been reported for **1**.[2]

Crystallographically, **2** is much flatter than **1**, with a biannular dihedral angle of only 14.5° due to an internal N(2)–H···O(3)–N(3) hydrogen bond from the uradinyl to the iminoylnitroxide moiety (dashed bond, Fig. 1). The radical forms two-point hydrogen bonded dimers, pairs of which are related through offset, inverted π-stacking between the uradinyl and iminoylnitroxide moieties (Fig. 2). The uradinyl rings are

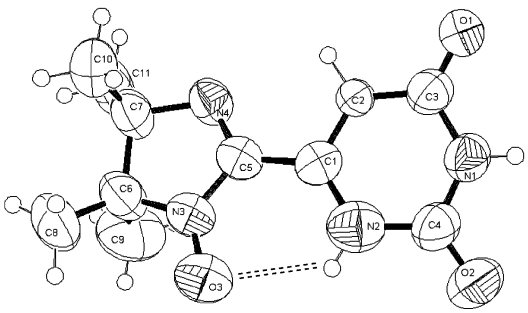

Fig. 1 ORTEP diagram for **2**. See the electronic supporting information for more crystallographic details. Dashed line shows a NH···ON internal hydrogen bond.

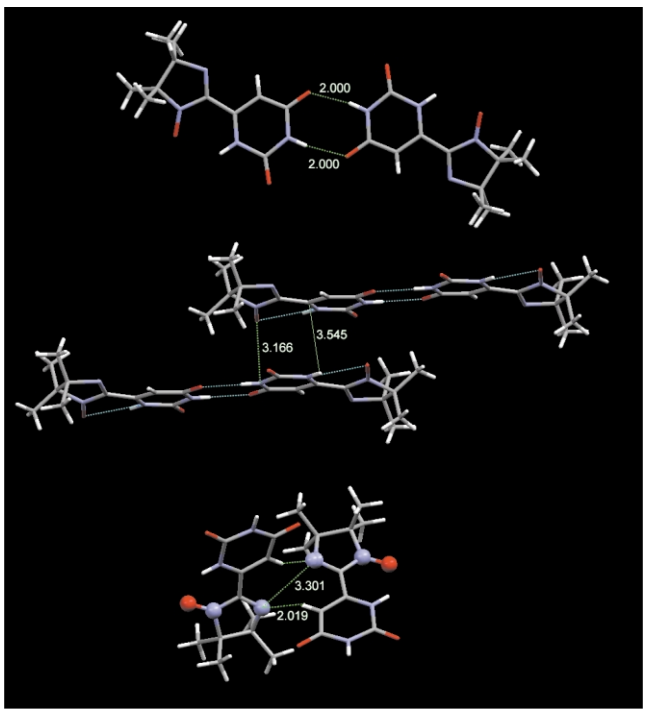

Fig. 2 Crystal structure of **2** showing the hydrogen-bonded dimers, π-stacking, and close contacts between sites of significant spin density. Distances are shown in angstroms.

† Electronic supplementary information (ESI) available: synthesis details for **1** and **2**; IR data; spin density computations for **2**. See http://www.rsc.org/suppdata/cc/b3/b302901h/

DOI: 10.1039/b302901h

stacked at a distance of about 3.5 Å, with the iminoylnitroxide N–O(3) lying about 3.2 Å above a uradinyl ring below it.

DC magnetic susceptibility measurements for **2** were carried out using a Quantum Design MPMS SQUID magnetometer over a range of 1.8–300 K at 1000 Oersted. Fig. 3 shows χ *vs.* T plots for the diamagnetism-corrected paramagnetic susceptibility (χ) data obtained. There are substantial deviations from linear Curie–Weiss behavior below 15 K indicating antiferromagnetic interactions between spin sites. The limiting behavior Curie constant $C = 2.75$ mol Oe^{-1} emu^{-1} with Weiss constant $\theta = -0.43$ K for $T > 80$ K, consistent with the value of $C = 2.67$ expected for $S = \frac{1}{2}$ spin units. The χ *versus* T data was fit to equation (1),

$$\chi = P \cdot \frac{C}{[T-\theta]} + (1-P) \cdot \frac{D/(T-\theta)}{3+\exp(-2J/T)} \qquad (1)$$

$$C = \frac{Ng^2\mu_B^2}{4k}, D = \frac{Ng^2\mu_B^2}{k}$$

in which N = Avogadro's number, μ_B = Bohr magneton, k = Boltzmann's constant, J is the exchange constant for spin pairing, and θ is a mean field interaction term. The equation provides for a small fraction of isolated spins (P) acting in a paramagnetic fashion. A good fit was obtained for $J/k = -7.0$ K (P optimized to 0.03) to -6.4 K (P fixed at zero), with a fixed value of $\theta = -0.43$ K from the high temperature Curie–Weiss plot. Fig. 3 shows the plot where P is fitted to the data.

The antiferromagnetic (AFM) spin pairing in **2** can be explained in terms of close contacts between sites of significant spin density (Fig. 2). The imine nitrogens (N(4)) of adjacent molecules are separated by 3.301 Å, providing the closest interatomic contact between sites of major spin density (the experimental $a_N = 4.6$ G, roughly a 15% spin population).[6] Although the N(4)···HC(2) contact is even closer (about 2.0 Å), the electron spin resonance (ESR) spectrum showed no resolvable hyperfine coupling attributable to the uradinyl H–C(2) bond. UBLYP[7]/cc-pVDZ[8] computations[9] at the experimental geometry of **2** show only (−)2% Mulliken spin density on C(2). Other atoms on the uradinyl ring are computed to have even smaller spin densities. Based on the computational and experimental evidence, it is likely that the 2-point dimeric hydrogen-bonds provide structural scaffolding, but not an electronic exchange pathway, given the small spin densities involved. The dimeric spin pairing appears primarily to be due to the close N(4)···N(4′) contacts shown in Fig. 2 (bottom).

Compounds such as **1–2** are of interest not only as components of molecular magnetic materials, but also as biorecognition agents. The strategies are related, since both biological and materials science techniques use directed molecular interactions (such as hydrogen bonding) to promote predictable molecular assemblages. The fine-tuning of primary structure features, such as the planarity of **2** by comparison to that of **1**, allows alteration of intermolecular behavior. In particular, we hope that the flat geometry of **2** will allow it to be deployed in work that we are pursuing with mixed crystals and in solution bio-recognition systems that have hydrogen bonding complementary to the uradinyl unit.

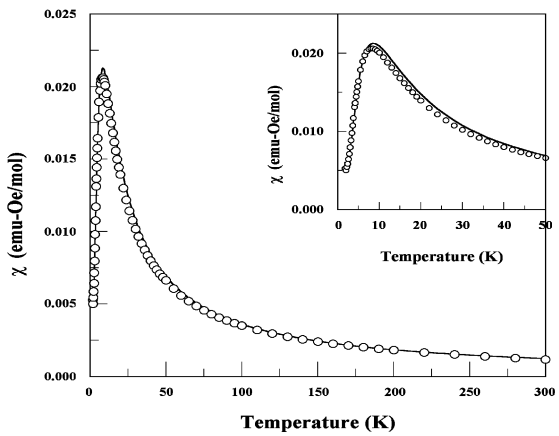

Fig. 3 Paramagnetic susceptibility (χ) *vs*. temperature for **2**. The solid line shows the fit of the data to equation 1. The inset shows the 0–50 K data and fit.

This work was supported by the National Science Foundation (NSF CHE-0109094). Magnetic measurements for **2** were obtained at the UMass-Amherst Nanomagnetics Characterization Facility (NSF CTS-0116498). The authors thank Dr. A. Chandrasekaran of the University of Massachusetts Amherst X-ray Structural Characterization Center (NSF CHE-9974648) for assistance with crystallographic analyses, Mr. Jonathan Wilson for assistance with mass spectrometry (University of Massachusetts Amherst Mass Spectrometry and Molecular Weight Determination Facility), and Dr. G. Dabkowski for elemental analyses.

Notes and references

‡ *Data for* **2**: mp 186–188 °C[d]. Anal. calc. for $C_{11}H_{15}N_4O_3$: C 52.58, H 6.02, N 22.30. Found: C 52.81, H 6.07, N 20.47%. MS (ESI, *m*/*z*): 252 (parent + H). ESR (9.645 GHz, chloroform): $a_N = 8.67$, 4.58 Gauss. Red needles from layered 1 : 1 CH_2Cl_2/H_2O. FTIR (KBr/cm^{-1}): 3423 (broad, NH), 3175, 3051, 2923 2830 (CH stretch), 1716, 1686 (amide N–C=O modes), 1412.

Crystal data for **2**, reddish cube, 0.35 × 0.35 × 0.20 mm, $C_{11}H_{15}N_4O_3$, $M = 251.26$, monoclinic, space group $C2/c$, $Z = 8$, $a = 13.3744(9)$, $b = 13.6012(9)$, $c = 15.1086(13)$ Å, $\beta = 109.701(3)°$, $V = 2587.5(3)$ Å^3, $D_{calc} = 1.290$ g cm^{-3}, $T = 298$ K, λ(Mo-Kα) = 0.7107 Å, $\mu = 0.096$ mm^{-1}. 4041 reflections were recorded at a threshold intensity of $2\sigma(I)$. 2244 independent reflections ($R_{int} = 0.0249$) were analyzed with 163 parameters using SHELXL-97. The final $R(F^2) = 0.086$, $wR(F^2) = 0.242$, R(all) = 0.111, wR(all) = 0.267. CCDC reference number 207264. See http://www.rsc.org/suppdata/cc/b3/b302901h/ for crystallographic data in CIF or other electronic format.

1 (*a*) J. Cirujeda, L. E. Ochando, J. M. Amigo, C. Rovira, J. Rius and J. Veciana, *Angew. Chem., Int. Ed. Engl.*, 1995, **34**, 55–57; (*b*) J. Cirujeda, E. Hernàndez-Gasió, C. Rovira, J.-L. Stanger, P. Turek and J. Veciana, *J. Mater. Chem*, 1995, **5**, 243–252; (*c*) T. Sugano, M. Tamura and M. Kinoshita, *Synth. Met.*, 1993, **55–57**, 3305–3310; (*d*) K. Awaga, T. Inabe, Y. Maruyama, T. Nakamura and M. Matsumoto, *Synth. Met.*, 1993, **55–57**, 3311–3316; (*e*) T. Sugawara, M. M. Matsushita, A. Izuoka, N. Wada, N. Takeda and M. Ishikawa, *J. Chem. Soc., Chem. Commun.*, 1994, 1723; (*f*) N. Yoshioka, N. Matsuoka, M. Irisawa, S. Ohba and H. Inoue, *Mol. Cryst. Liq. Cryst. Sci. Technol., Sect. A*, 1999, **334**, 239–246; (*g*) P. M. Lahti, J. R. Ferrer, C. George, P. Oliete, M. Julier and F. Palacio, *Polyhedron*, 2001, **20**, 1465–1473.

2 R. Feher, D. B. Amabalino, K. Wurst and J. Veciana, *Mol. Cryst. Liq. Cryst.*, 1999, **334**, 333–345.

3 M. Botta, F. De Angelis, F. Corelli, M. Menichincheri, R. Nicoletti, M. Marongiu, A. Pani and P. La Colla, *Arch. Pharm. (Weinheim)*, 1991, **324**, 203–207.

4 V. Ovcharenko, S. Fokin and P. Rey, *Mol. Cryst. Liq. Cryst.*, 1991, **334**, 109–119.

5 D. Maspoch, L. Catala, P. Gerbier, D. Ruiz-Molina, J. Vidal-Gancedo, K. Wurst, C. Rovira and J. Veciana, *Chem. Eur. J.*, 2001, **8**(16), 3635–3645.

6 *Cf*. the discussion in J. A. Pople and D. A Beveridge, *Approximate Molecular Orbital Theory*, McGraw-Hill, New York, NY, 1970, pp. 128–149. We used $|Q| = 30$ Gauss in the equation a(hfc) = $Q\rho$, where a(hfc) is the experimental nitrogen hyperfine coupling and ρ is the estimated corresponding spin population.

7 A. D. Becke, *J. Chem. Phys.*, 1993, **98**, 5648–5652.

8 D. E. Woon and T. H. Dunning, Jr., *J. Chem. Phys.*, 1993, **98**, 1358.

9 Computations were carried out using Gaussian 98: M. J. Frisch, G. W. Trucks, H. B. Schlegel, P. M. W. Gill, B. G. Johnson, M. A. Robb, J. R. Cheeseman, T. Keith, G. A. Petersson, J. A. Montgomery, K. Raghavachari, M. A. Al-Laham, V. G. Zakrzewski, J. V. Ortiz, J. B. Foresman, J. Cioslowski, B. B. Stefanov, A. Nanayakkara, M. Challacombe, C. Y. Peng, P. Y. Ayala, W. Chen, M. W. Wong, J. L. Andres, E. S. Replogle, R. Gomperts, R. L. Martin, D. J. Fox, J. S. Binkley, D. J. Defrees, J. Baker, J. P. Stewart, M. Head-Gordon, C. Gonzalez and J. A. Pople, in *Gaussian 98*, Pittsburgh, PA, 1998.